EURASIAN PHYSICAL TECHNICAL JOURNAL

2024, Volume 21, No.4 (50)

https://doi.org/10.31489/2024No4/99-108

Received: 07/06/2024 Revised: 11/10/2024 Accepted: 13/12/2024 Published online: 25/12/2024

Original Research Article

Open Access under the CC BY -NC-ND 4.0 license

UDC 539.374.1, 539.381, 539.4.012, 621.735.3:621.983.31

MODELING IN THE DESIGN OF TECHNOLOGICAL PROCESSES FOR DRAWING WITH WALL THINNING OF HOLLOW AXISYMMETRIC PARTS FOR VARIOUS PURPOSES

Rasulov Z.[1], Olehver A.[1], Remshev E.[1], Voinash S.[2], Vornacheva I.[3], Sokolova V.[2], Malikov V.[4]*

[1] Baltic State Technical University "Voenmeh" named after D.F. Ustinov, Saint Petersburg, Russia

[2] Kazan Federal University, Kazan, Russia

[3] South-West State University, Kursk, Russia

[4] Altai State University, Barnaul, Russia

*Corresponding author: osys11@gmail.com

Abstract. *There are a number of products that operate under extremely difficult conditions of complex loading, the manufacture of which by traditional stamping operations does not provide the required properties, which leads to a large number of defects. One of the possible directions for the manufacture of products of increased strength is the introduction into the technological process of methods of intense plastic deformation, which can be either volumetric (equal-channel angular pressing, longitudinal extrusion through a channel of variable cross-section, drawing with wall thinning along the internal contour) or surface (grinding holes, rolling with rollers or balls). The study demonstrates the application of the approximate monotonicity criterion and its relationship with technological parameters, using the example of a deep drawing process with wall thinning. A case is presented where technological parameters, including friction conditions and the degree of deformation, are selected to ensure approximate monotonicity during the thinning process. The findings provide a basis for the rational selection of the "strain-stress" curve, contributing to a more accurate and efficient design of deformation processes.*

Keywords: Technological process, drawing with wall thinning, intense plastic deformation, criterion of approximate monotonicity, stress-strain state.

1. Introduction

The solution of metal forming problems through the calculation of the stress-strain state (SSS) is based on several assumptions, one of which involves adopting a specific "strain-stress" curve. According to the established classification of complex loading processes [1-9], the selection of this curve is intricately linked to the concept of monotonic deformation, a term introduced into scientific discourse by G.A. Smirnov-Alyaev [2]. This process is widely used in the manufacture of axisymmetric parts with constant and variable wall thickness [3–4]. The deforming elements are a cylindrical mandrel and a roller having a conical or torus shape. During processing, the roller rolls along a rotating workpiece with a given axial feed and ensures forced thinning of the wall to the required value. Within the geometric focus of deformation, the material is under conditions of uneven all-round compression, which greatly complicates the theoretical study of the SSS of this process. This determines that the improvement of the technology of the rotary drawing process is based mainly on the results, on the basis of which various theoretical models are developed [5–10].

The purpose – is to apply the approximate monotonicity criterion and establish its connection with technological parameters using the example of a hood with wall thinning, to develop an algorithm for selecting technological parameters, such as friction conditions and the degree of deformation, in the thinning process of a deep drawing operation is designed to ensure the approximate monotonicity of the process. This algorithm provides a systematic approach to optimizing the deformation process by maintaining stability in the strain distribution and minimizing deviations from monotonic behavior throughout the operation.

The results allow a reasonable choice of the “strain-stress” curve.

Monotonic deformation is characterized by the simultaneous fulfillment of two conditions:

1) the principal axes of the strain rate remain aligned with the same material fibers throughout the process;

2) the value of $\nu = \nu_{\dot{\varepsilon}} = \frac{2\dot{\varepsilon}_2 - \dot{\varepsilon}_1 - \dot{\varepsilon}_3}{\dot{\varepsilon}_1 - \dot{\varepsilon}_3}$ remains constant during the entire deformation.

The first condition of monotonicity means the coaxiality of the tensors T_ε and $T_{\dot{\varepsilon}}$. In other words, if denote the principal axes of tensor T_ε as X_1, X_2 and X_3 corresponding to its eigenvalues $\lambda_1 > \lambda_2 > \lambda_3$, and the principal axes of tensor $T_{\dot{\varepsilon}}$ as Y_1, Y_2 and Y_3 – then the relationships $X_1||Y_1$, $X_2||Y_2$ and $X_3||Y_3$ must hold.

Let us denote the rotation angle of the principal axes of the strain rate tensor relative to the principal axes of the strain tensor as α. he first condition for monotonicity can then be expressed as $\alpha = 0$. The second condition, by definition, is written as ν =const.

For any given process, the selection of the "strain-stress" curve depends on whether both conditions are fully met, only one is satisfied, or neither holds true [1].

In practice, however, the exact fulfillment of $\alpha = 0$ and ν =const, is unlikely, as these are idealized equality conditions. When addressing real-world problems, the concept of "approximate monotonicity" is typically used, although the degree of this approximation is not explicitly quantified. In general, both α and ν ary over time, expressed as $\alpha = \alpha(t)$, $\nu = \nu(t)$.

In [1], a criterion for approximate monotonicity was proposed:

$$d = max\left[\frac{1}{\pi}\max_t(\alpha(t)); \frac{1}{2}\left(\max_t \nu(t) - \min_t \nu(t)\right)\right] \quad (1)$$

- a scalar, based on the value of which you can decide whether or not to consider a given process monotonic. The criterion for approximate monotonicity d y satisfies the inequality $0 \le d \le 1$, and for monotonic processes the equality $d = 0$ holds.

The concept of monotonic deformation by Smirnov-Alyaeva G.A. establishes a connection between the strain tensor and the strain rate tensor. The use of flow theory in solving plastic deformation problems in metal forming focuses on quantities such as flow rates, strain rates, and stresses, without involving displacements or deformations in the solution. Conversely, when the theory of small elastic deformations is applied, the analysis excludes velocities and strain rates, focusing instead on displacements and deformations.

In [11], which develops this approach, the strain rate is determined using sections in accordance with a methodology in which the deformed state is determined using microstructural analysis performed near a selected point. The authors conducted a drawing and deformation study in which a single cold drawing pass drew a 12 mm diameter circular tube with a 1 mm wall thickness made of steel into a square tube. This study determined how material properties affect the energy intensity of the manufacturing process and the strain rate when drawing a square tube.

The development of deformations has been studied in a number of other works. Khatala et al. [12] studied the deformations that occur in a non-circular pipe during processing and described the development of a mathematical model using the DEFORM software package. State variables describing the initial state of the material (such as stress, strain, and strain rate) and the flow of material during the drawing process were determined through numerical calculation. Boutenel et al. [13] studied the cold drawing of high-precision non-circular pipes using a computer model that very accurately predicted the final dimensions of the pipe and determined the effect of die angle on the drawing force and the effect of relative thickness on pipe deformation.

In [14], under a number of assumptions (including the plane nature of the problem), the stress-strain state (SSS) of the workpiece wall during drawing with thinning was calculated. The expression for the

intensity of the strain rate is the product of two functions that depend on only one variable and has a relatively simple form.

In the event that the expression for the intensity of the strain rate does not have a simple form, constructing an analytical solution to the system of equilibrium equations is very difficult. The assumption of the flat nature of the problem adopted in [14, 15] is quite restrictive for cartridge-case production, since the ratio of the wall thickness of the semi-finished case to its diameter is quite large, so it is necessary to classify the case as a thick-walled workpiece. It is also impossible to use the obtained solution for calculating the stress-strain state and assessing the degree of deformation of thick-walled workpieces during drawing with thinning. Blanks for drawing with thinning are divided into thin-walled and thick-walled blanks.

2. Practical Research

Let us demonstrate the practical application of the approximate monotonicity criteria using the example of a hood with wall thinning. In [3], a flow velocity field was constructed for drawing with thinning. Under the assumptions made there, the zone of plastic deformation (ZPD) has the form of an annular sector limited by circles of radii $r = a$ and $r = b$ $(a < b)$, angular valueγ. The speeds are:

$v_r = \frac{f(\phi)}{r}$, $v_\phi = 0$, $v_\theta = 0$,

where $f(\phi)$ was calculated in [4]:

$$f(\phi) = -v_0 a \cdot e^{\frac{2}{C\sqrt{3}}\left(\sqrt{1-3{C_1}^2}-\sqrt{1-3(C_1-C\phi)^2}\right)} \tag{2}$$

and satisfies the inequality $f(\phi) < 0$. Thus, the movement of particles along the ZPD occurs in the radial direction in the direction of decreasing the radius. This movement determines the unique dependence of the radial coordinate on time, the explicit form of which is established in [4]:

$$t(\phi) = \frac{r^2-b^2}{2\cdot f(\phi)}. \tag{3}$$

By definition of current speed $v_r = \frac{du_r}{dt}$. Writing the speed v_r taking into account (3) as a function of time, find:

$$u_r = \int_0^t \frac{f(\phi)dt}{\sqrt{b^2+2t\cdot f(\phi)}} = \sqrt{b^2 + 2t \cdot f(\phi)} - b. \tag{4}$$

Note that take into account relation (3) in relation (4), obtain $u_r = r - b$, as one would expect. It's obvious that $u_\phi = 0$, $u_\theta = 0$. Knowing the displacements, calculate the deformations: $\varepsilon_r = 1$, $\varepsilon_\phi = \frac{r-b}{r}$. To search for shear strain $\gamma_{r\phi}$ use relation (4):

$$\gamma_{r\phi} = \frac{1}{r}\frac{t\cdot f'(\phi)}{\sqrt{b^2+2t\cdot f(\phi)}} = \frac{(r^2-b^2)\cdot f'(\phi)}{2r^2\cdot f(\phi)} \tag{5}$$

Thus, the strain tensors T_ε and strain rate $T_{\dot\varepsilon}$ (its components are taken from [3]) have the form:

$$T_\varepsilon = \begin{pmatrix} 1 & \frac{(r^2-b^2)\cdot f'(\phi)}{2r^2\cdot f(\phi)} & 0 \\ \frac{(r^2-b^2)\cdot f'(\phi)}{2r^2\cdot f(\phi)} & \frac{r-b}{r} & 0 \\ 0 & 0 & 0 \end{pmatrix} \text{ and } T_{\dot\varepsilon} = \begin{pmatrix} -\frac{f(\phi)}{r^2} & \frac{f'(\phi)}{2r^2} & 0 \\ \frac{f'(\phi)}{2r^2} & \frac{f(\phi)}{r^2} & 0 \\ 0 & 0 & 0 \end{pmatrix}. \tag{6}$$

The inequalities are satisfied (in the first one must take into account that $\frac{r-b}{r} < 0$):

$$det\begin{pmatrix} 1 & \frac{(r^2-b^2)\cdot f'(\phi)}{2r^2\cdot f(\phi)} \\ \frac{(r^2-b^2)\cdot f'(\phi)}{2r^2\cdot f(\phi)} & \frac{r-b}{r} \end{pmatrix} < 0, \quad det\begin{pmatrix} -\frac{f(\phi)}{r^2} & \frac{f'(\phi)}{2r^2} \\ \frac{f'(\phi)}{2r^2} & \frac{f(\phi)}{r^2} \end{pmatrix} < 0.$$

As a result, the eigenvalues of both tensors T_ε and $T_{\dot{\varepsilon}}$ include one positive, one zero, and one negative value, with the zero-eigenvalue corresponding to the eigenvector $(0 \quad 0 \quad 1)$ for both tensors. Consequently, the first and third principal axes of one tensor are generally rotated by a certain angle in the *XOY* plane relative to the corresponding axes of the other tensor. This angle is denoted as α. It is important to note that the presence of a zero eigenvalue, combined with the incompressibility condition (i.e., the zero trace condition for the tensor $T_{\dot{\varepsilon}}$) implies that $\nu = 0$. Therefore, the second condition of monotonicity is satisfied, and the expression for the measure of monotonicity becomes $d = \frac{1}{\pi} \underset{t}{max}(\alpha(t))$.

To compute the angle α between the first principal vectors of two matrices, it is advantageous for the matrices to be in their simplest form. According to the definitions of eigenvalues and eigenvectors, if X is an eigenvector of matrix A, corresponding to the eigenvalue λ, then for any $\mu \in (-\infty; +\infty)$ the vector X is an eigenvector of matrix $A + \mu E$ (where E is the identity matrix), corresponding to the eigenvalue $\lambda + \mu$.

Furthermore, when substituting matrix A with $A + \mu E$ t the order of the eigenvalues remains unchanged; thus, the largest eigenvalue of matrix A corresponds to the largest eigenvalue of matrix $A + \mu E$. Additionally, scaling a matrix by any positive constant does not affect the order of its eigenvalues or the corresponding eigenvectors. This property allows for the transformation of matrices T_ε and $T_{\dot{\varepsilon}}$ into matrices of a simpler structure. The original matrices T_ε and $T_{\dot{\varepsilon}}$ are represented as follows (see (6)):

$$T = \begin{pmatrix} c_{11} & c_{12} & 0 \\ c_{12} & c_{22} & 0 \\ 0 & 0 & 0 \end{pmatrix}$$

Let us denote the matrix obtained by this transformation from T_ε, by A, and the matrix obtained from $T_{\dot{\varepsilon}}$, by B:

$$A = \begin{pmatrix} 1 & a_{12} & 0 \\ a_{12} & -1 & 0 \\ 0 & 0 & a_{33} \end{pmatrix}, \quad B = \begin{pmatrix} 1 & b_{12} & 0 \\ b_{12} & -1 & 0 \\ 0 & 0 & 0 \end{pmatrix},$$

here

$$a_{12} = -\frac{2(b^2-r^2)}{rb} \cdot \frac{f'(\phi)}{2f(\phi)} \text{ и } b_{12} = -\frac{f'(\phi)}{2f(\phi)} \tag{7}$$

Note that b_{12} is a function only of the angle ϕ, that is, b_{12} does not change on a fixed trajectory. Note also that $a_{12} = \frac{2(b^2-r^2)}{rb} \cdot b_{12}$. The value $k = \frac{2(b^2-r^2)}{rb}$ is a certain coefficient of proportionality that depends only on the radius r, that is, changing along any fixed trajectory. Since $a \le r \le b$, then the coefficient k is positive. Moreover, since

$$k_r' = \left(\frac{2(b^2-r^2)}{rb}\right)' = -\frac{2(b^2+r^2)}{br^2} < 0,$$

then the coefficient k is a monotonically decreasing function of r, that is, when moving along the trajectory towards a decreasing radius, the coefficient k monotonically increases.

Thus, to calculate the approximate monotonicity criteria, it remains to calculate the angle α between the first eigenvectors X_1 and Y_1 matrices A and B. The angle α_1 between X_1 and the OX axis:

$$\alpha_1 = \text{arctg}\frac{a_{12}}{1+\sqrt{1+a_{12}^2}} = \frac{\text{arctg}(a_{12})}{2}.$$

Similarly, the angle α_2 between Y_1 and the OX axis:

$$\alpha_2 = \text{arctg}\frac{b_{12}}{1+\sqrt{1+b_{12}^2}} = \frac{\text{arctg}(b_{12})}{2}.$$

Consequently, $\alpha = |\alpha_1 - \alpha_2|$. Along any fixed trajectory, the angle α_2 remains constant. When $r = b$ (at the entry point to the ZPD), the condition $k = 0$ is fulfilled, resulting in $a_{12} = 0$, which indicates that X_1 aligns with the *OX* axis, making the desired angle $\alpha = \alpha_2$. The diagram illustrating the variation of angle α The diagram illustrating the variation of angle $k = 1$, matrices A and B will be identical, leading to the condition $\alpha = 0$.

By solving the equation $k = 1$, obtain the corresponding value $r_0 = \frac{\sqrt{17}-1}{4}b$). With a further increase in the coefficient k the angle α_1, which has already exceeded the angle α_2, will continue to increase, so it will be $\alpha = \alpha_1 - \alpha_2$. At some point, the equality $\alpha_1 = 2\alpha_2$, will be achieved, at which again $\alpha = \alpha_2$ will appear (by solving the equation $\alpha_1 = 2\alpha_2$, find that for $|b_{12}| < 1$ a solution exists, the corresponding coefficient $k = \frac{2}{1-b_{12}^2}$, and the radius value

$$r_1 = \frac{\sqrt{4b_{12}^4 - 8b_{12}^2 + 5} - 1}{2(1 - b_{12}^2)}b$$

(whereby the inequality $r_1 < r_0$ always holds, and for $|b_{12}| \geq 1$ the equality $\alpha_1 = 2\alpha_2$ is impossible). The value of the internal radius a determines to what value the radius will decrease when moving along the trajectory in the ZPD. There are three options:

1) if $r_0 < a$ (such a in Fig.1 is designated as a_1), then $min\,\alpha = \alpha_2 - \alpha_1(a_1)$, $max\,\alpha = \alpha_2 - \alpha_1(b) = \alpha_2$.

2) if $r_1 < a \leq r_0$ (such a in Fig.1 is designated as a_2), then $min\,\alpha = \alpha_2 - \alpha_1(r_0) = 0$, $max\,\alpha = \alpha_2 - \alpha_1(b) = \alpha_2$.

2) if $a \leq r_1$ (such a in Fig.1 is designated as a_3), then $min\,\alpha = \alpha_2 - \alpha_1(r_0) = 0$, $max\,\alpha = \alpha_1(a_3) - \alpha_2$.

It follows that on each fixed trajectory, if the thickness of the ZPD in the radial direction is not too large, then $d = \frac{1}{\pi}\alpha_2$ is achieved at the entrance to the ZPD, and if the thickness of the ZPD in the radial direction is sufficiently large, then $d = \frac{1}{\pi}(\alpha_1(a) - \alpha_2) > \frac{1}{\pi}\alpha_2$ and is achieved at the exit from the ZPD.

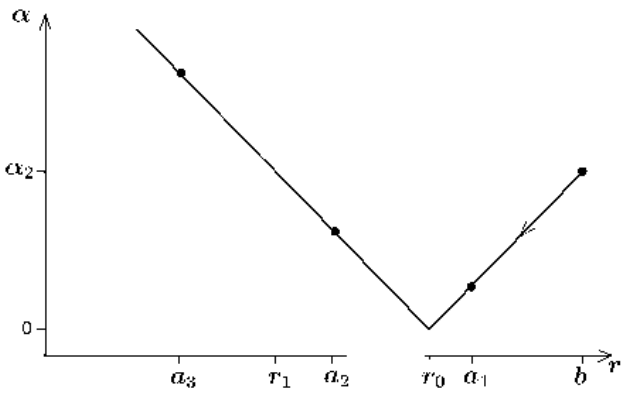

Fig.1. Variation of the angle $\boldsymbol{\alpha}$ while traversing along a trajectory is observed at point $\boldsymbol{r = b}$ — which serves as the entry point into the ZPD. The points $\boldsymbol{a_1}$, $\boldsymbol{a_2}$, $\boldsymbol{a_3}$ represent potential exit points from the ZPD, corresponding to different values of the internal radius of the ZPD under varying degrees of deformation and friction conditions.

In both cases, the angle α_2 (and, therefore, the value of d) depends on the angle ϕ f the entrance to the ZPD and the friction coefficients along the working surfaces of the punch and matrix. Let us establish this dependence explicitly. Substituting explicit expression (2) for the function $f(\phi)$ into formula (7), after transformations obtain (here $C_1 = 0.5\beta\mu_1$, $C = \frac{\beta(0.5\mu_1 - \mu)}{\alpha}$, μ is the friction coefficient on the surface matrix, μ_1 is coefficient of friction on the surface of the punch (the law of constant friction force is applied (Siebel's law, or Prandtl's law), therefore $0 \leq \mu \leq 0.5$ и $0 \leq \mu_1 \leq 0.5$), α is cone angle of the matrix drawing particle):

$b_{12} = \frac{(C_1 - C\phi)\sqrt{3}}{\sqrt{1-3(C_1-C\phi)^2}}$.

If denote $Q = C_1 - C\phi$ (the value of Q reflects the cumulative influence of friction coefficients), and take into account that $0 \le min(\beta\mu_1/2; \beta\mu) \le Q \le max(\beta\mu_1/2; \beta\mu) \le 1/\sqrt{3}$, then the value

$$\alpha_2 = \frac{\text{arctg}(b_{12})}{2} = \frac{1}{2}\text{arctg}\frac{Q\sqrt{3}}{\sqrt{1-3Q^2}}$$

monotonically increases from 0 to $\pi/4$. In order for the inequality $|b_{12}| < 1$ to be satisfied, it is necessary and sufficient to satisfy the inequality $\frac{Q\sqrt{3}}{\sqrt{1-3Q^2}} < 1$, from which obtain $|Q| < 1/\sqrt{6}$ (for such Q there will be $\alpha_2 < \pi/8$). In this case have: $r_1 = \frac{\sqrt{153Q^4-54Q^2+5}-(1-3Q^2)}{2(1-6Q^2)}b$. Graphs of α_2 and r_1/b as functions of Q are shown in Fig.2.

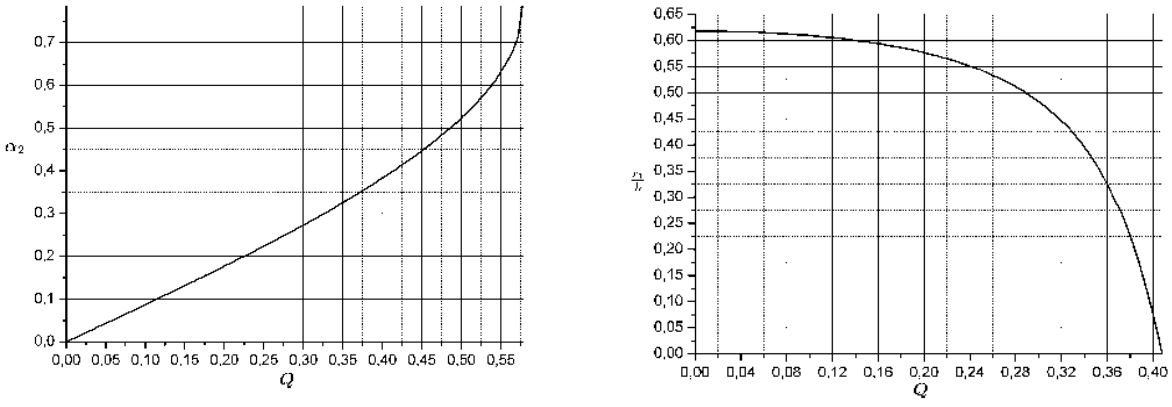

a) b)

Fig.2. a) Dependence of angle α_2 (in radians) on Q; б) Dependence of the value r_1/b on Q

So, will show how to evaluate the monotonicity of the drawing process with wall thinning.

First, let us consider the problem of selecting technological parameters so that the deformation can be considered approximately monotonic. Establish the threshold value for the criterion of approximate monotonicity as $d_n = \frac{1}{18}$ which corresponds to an allowable deviation of the principal axes of the deformation tensor from one another by an angle not exceeding 10°. Assume that if the inequality $d \le d_n$, is satisfied, the process can be considered monotonic; conversely, if $d > d_n$ monotonicity cannot be guaranteed. This threshold value d_n corresponds to $\alpha_{2n} = \pi \cdot d_n = 0.17453$. Based on the relationship between the angle α_2 от Q (see Fig. 2a), calculate the threshold value:

$$Q_n = \frac{1}{\sqrt{3}}sin(2\alpha_{2n}) = \frac{1}{\sqrt{3}}sin\frac{\pi}{9} = 0.19747.$$

Then the limits are achieved by the coefficient of friction:

$$max(\beta\mu_1/2; \beta\mu) \le \frac{1}{\sqrt{3}}sin\frac{\pi}{9} \Leftrightarrow \begin{cases} \mu_1 \le \frac{2}{\beta\sqrt{3}}sin\frac{\pi}{9} \approx 0.34202, \\ \mu \le \frac{1}{\beta\sqrt{3}}sin\frac{\pi}{9} \approx 0.17101. \end{cases} \quad (8)$$

Moreover, since $Q_n < 1/\sqrt{6} \approx 0.40825$ (that is, $|b_{12}| < 1$), then, depending on the extent of deformation, any of the three cases is possible (which correspond to points a_1, a_2, a_3 of the exit from the ZPD). To obtain case 1 from the inequality $r_0 < a$ and formulas for the radii of the OPD [3, p. 279, (15.23)] $b = (R_{нд} - r_в)/sin(\gamma)$ and $a = (R_{нп} - r_в)/sin(\gamma)$ (here $R_{нд}$ is the outer radius before drawing with thinning, $R_{нп}$ is the outer radius after drawing, $r_в$ is inner radius, γ is cone angle of the exhaust part of the matrix) find that $R_{нп}$ should not be too small, that is, the degree of deformation should not be too big:

$$R_{нп} > \frac{\sqrt{17}-1}{4} R_{нд} + \frac{5-\sqrt{17}}{4} r_в \approx 0.78078 R_{нд} + 0.21922 r_в.$$

To obtain case 2, firstly, it is required that $R_{нп}$ be small enough

$$r_в < R_{нп} \leq \frac{\sqrt{17}-1}{4} R_{нд} + \frac{5-\sqrt{17}}{4} r_в \approx \approx 0.78078 R_{нд} + 0.21922 r_в$$

(the degree of deformation must be quite large), and, secondly, the inequality $r_1 < a$, must be satisfied, that is:

$$\frac{\sqrt{153Q^4-54Q^2+5}-(1-3Q^2)}{2(1-6Q^2)} (R_{нд} - r_в) + r_в < R_{нп}.$$

To obtain case 3, firstly, the inequality is required

$$r_в < R_{нп} < \frac{\sqrt{153Q^4-54Q^2+5}-(1-3Q^2)}{2(1-6Q^2)} (R_{нд} - r_в) + r_в,$$

and, secondly, since in case 3 $max\,\alpha = \alpha_1(a_3) - \alpha_2$, s satisfied, then for approximate monotonicity it should be $max\,\alpha = \alpha_1(a_3) - \alpha_2 \leq \frac{\pi}{18} \approx 0.17453$, that is

$$max\,\alpha = \alpha_1(kb_{12}) - \alpha_2 = \frac{1}{2}\text{arctg}(kb_{12}) - \frac{1}{2}\text{arctg}(b_{12}) \leq \frac{\pi}{18}.$$

Thus, if need to get it an approximately monotonic drawing with wall thinning, it is necessary to set the value of the radius R_{np} (the radii R_{nd}, r_v can be regarded as fixed parameters, allowing the selection of R_{np} to uniquely determine the resulting degree of deformation while ensuring that the friction coefficients remain at acceptable (relatively low) levels. Depending on the relative values of the radii R_{nd}, R_{np}, r_v an approximately monotonic drawing will be achieved in one of the scenarios outlined in cases 1-3.

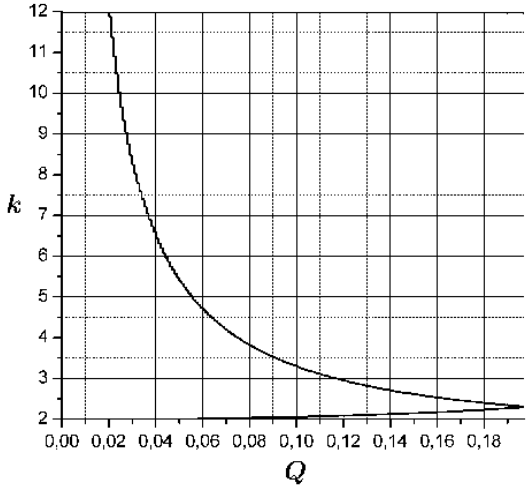

Fig.3. Admissible values of parameters Q and k (located to the left of the curve), at which the third case of approximate monotonicity is realized.

To address the inverse problem of determining whether a specific hood with a thinning wall can be classified as monotonic, it is essential to first evaluate the range of values for Q: $min(\beta\mu_1/2;\ \ \beta\mu) \leq Q \leq max(\beta\mu_1/2;\ \ \beta\mu)$. Next, the angle α_2 should be calculated (or estimated from Fig. 2a). If the resulting angle $\alpha_{2n} = 0.17453$, the drawing cannot be considered monotonic. Conversely, if the inequality $\alpha_2 \leq \alpha_{2n} = 0.17453$ holds true, it is then necessary to compute (or estimate from Fig. 2b) the value of r_1. Now, using the known outer radius of the part before drawing $R_{нд}$, the outer radius after drawing $R_{нп}$, the inner

radius $r_в$ and the taper angle γ it is necessary to calculate the outer b and inner radii a of the ZPD and check the inequality $a \geq r_1$. f this is done, then the hood can be considered monotonous. If the inequality $a < r_1$, is satisfied, then it is necessary to check the fulfillment of the inequality

$$\frac{1}{2}\operatorname{arctg}\left(\frac{2(b^2-a^2)}{ab}\frac{Q\sqrt{3}}{\sqrt{1-3Q^2}}\right) - \frac{1}{2}\operatorname{arctg}\frac{Q\sqrt{3}}{\sqrt{1-3Q^2}} \leq \frac{\pi}{18}. \quad (9)$$

If it is done, then the hood can be considered monotonous; if it is not done, then it cannot be.

3. Results and discussion

Let us consider the application of the above calculations to solve practical problems in the field of designing a working tool for a drawing operation with wall thinning:

Example 1. Let $R_{нд} = 40$ mm, $R_{нп} = 38.5$ mm, $r_в = 30$ mm, $\gamma = 2°$,$\mu = 0.1$, $\mu_1 = 0.1$. Calculate: $0.058 \leq Q \leq 0.115$, $0.05 \leq \alpha_2 \leq 0.101$. Since the inequality $\alpha_2 \leq \alpha_{2п} = 0.17453$ is satisfied, we calculate the range of variation of r_1: $173.7 \leq r_1 \leq 176.3$ and radii: $b = 286.5$mm, $a = 243.6$mm. Since the inequality $a \geq r_1$, holds, the drawing can be considered monotonic.

Example 2. Let $R_{нд} = 40$mm, $R_{нп} = 38.5$mm, $r_в = 30$mm, $\gamma = 2$, $\mu = 0.2$, $\mu_1 = 0.1$. Calculate: $0.058 \leq Q \leq 0.231$, $0.05 \leq \alpha_2 \leq 0.206$. Since some of the α_2 values exceed the threshold value $\alpha_{2п} = 0.17453$, the hood cannot be considered monotonic. This happened because the friction coefficient μ does not satisfy inequality (8). In general, inequalities (8) are the main conditions on which approximate monotonicity depends.

Example 3. Let $R_{нд} = 40$mm, $R_{нп} = 36$mm, $r_в = 30$mm, $\gamma = 2°$,$\mu = 0.1$, $\mu_1 = 0.1$. Calculate: $0.058 \leq Q \leq 0.115$, $0.05 \leq \alpha_2 \leq 0.101$. Since the inequality $\alpha_2 \leq \alpha_{2п} = 0.17453$ is satisfied, calculate the range of changes: r_1 : $173.7 \leq r_1 \leq 176.3$ and radii: $b = 286.5$mm, $a = 171.9$mm. Since the inequality $a < r_1$, it is necessary to check the fulfillment of inequality (9) over the entire range of changes in Q. For Q_{min}: $0.056 < \pi/18 \approx 0.175$ - fulfilled, for Q_{max}: $0.105 < \pi/18 \approx 0.175$ - fulfilled. Thus, the hood can be considered monotonous. It is necessary to check inequality (8) even if for part of the range of variation r_1 the inequality $a < r_1$ is satisfied, but for part it is not.

In the examined model, the parameters that define the geometric dimensions of the exhaust section of the matrix are the radii $R_{нд}$, $R_{нп}$ and $r_в$. Consequently, it can be concluded that approximate monotonicity is influenced by the cone angle solely through the radii b and a (similar to how the degree of deformation for the exhaust with wall thinning is calculated in [4]), given that any arbitrary matrix thickness (greater than 115 mm, as illustrated in example 3) is deemed acceptable. However, if the matrix thickness is treated as a fixed parameter, then a drawing with a significant degree of thinning will inherently necessitate a larger taper angle. Let's say, increasing the taper angle for the data from example 3 to $\gamma = 12$ (and keeping the remaining data), obtain $b = 48.1$mm, $a = 28.9$mm, $29.2 \leq r_1 \leq 29.6$ while keeping the ranges for Q and α_2 and the left sides of inequality (9) for Q_{min} and Q_{max} and with still approximately monotonic stretching.

4. Conclusion

In engineering technological practice, monotonic processes are rare. At the same time, a huge number of technological problems are associated with the analysis of processes close to monotonic, due to the limitations imposed on engineering calculation models. In this regard, an assessment of the proximity of a specific technological process being developed to a monotonic or other special cases of complex loading is necessary, since this allows us to assess the validity of using a particular rheological model of the processed material, which underlies this technological problem.

At the current stage of research, the developed technological recommendations allow the process engineer to assess the "level of monotonicity" of the process and, if necessary, make changes to the deformation modes of the semi-finished product. Providing the operation with the condition of a "monotonic" process allows us to minimize errors in the application of a rheological model of material hardening (for example, based on the results of a tensile test) and, thereby, predict the possibility of hardening the material and ensuring tactical and technical requirements, the possibility of loss of stability or destruction.

The result of the implementation of this tool is a stable technological process, where a balance is maintained between the level of material hardening acquired during stamping operations and heat treatment, which leads to a reduction in defects and an increase in the quality of manufactured products.

Conflict of interest statement

The authors declare that they have no conflict of interest in relation to this research, whether financial, personal, authorship or otherwise, that could affect the research and its results presented in this paper.

CRediT author statement

Rasulov Z.- Conceptualization, Methodology; **Olehver A**. - Software; **Voinash S.A. -** Validation; **Vornacheva I and Sokolova V**. - Writing - Review & Editing; **Malikov V.** - Supervision.
The final manuscript was read and approved by all authors.

Acknowledgements

This work was carried out with financial support from the Ministry of Science and Higher Education of the Russian Federation (research and development project "Research and prediction of gradient fields of strength and plastic characteristics of metals in cold forming processes under complex loading" FZWF-2024-0006).

References

1 Vinnik P.M., Ivanov K.M. (2016) Processes of complex loading in technological problems. *News of higher educational institutions. Mechanical engineering.* 6, 675, 62-72. Available at: https://www.researchgate.net/publication/308389554_ Combined_Loading_Processes_in_Technological_Problems

2 Smirnov-Alyaev G.A. (1978) Resistance of materials to plastic deformation. Leningrad, Mashinostroenie Publ., 368 p. Available at: https://studfile.net/preview/19957333/ [in Russian]

3 Haghshenas M., Klassen R.J. (2015) Mechanical characterization of flow formed FCC alloys. *Materials Science and Engineering,* 641, 249 – 55. DOI: 10.1016/j.msea.2015.06.046.

4 Bhatt R.J., Raval H.K. (2017) Investigation of effect of material properties on forces during flow forming process. *Procedia Engineering,* 173, 1587 – 1594. DOI: 10.1016/j.proeng.2016.12.265.

5 Davidson M.J., Balasubramanian K., Tagorea G.R.N. (2008) An experimental study on the quality of flowformed AA6061 tubes. *Journal of Materials Processing Technology*, 203 (1–3), 321 – 325. DOI:10.1016/j.jmatprotec.2007.10.021.

6 Bedekar V., Pauskar P., Shivpuri R. (2017) Microstructure and texture evolutions in AISI 1050 steel by flow forming. *J. HoweProcedia Engineering*, 81, 2355 – 2360. DOI: 10.1016/j. proeng.2014.10.333.

7 Marini D., Corney J. (2008) A methodology for assessing the feasibility of producing components by flow forming. *Journal of Materials Processing Technolog,* 5(1), 210–234. DOI: 10.1080/21693277.2017.1374888.

8 Wang X., Xia Q., Cheng X. (2017) Deformation behavior of Haynes 230 superalloy during backward flow forming. *Int. J. Precis. Eng. Manuf.*, 18(1), 77 – 83. DOI: 10.1007/s12541-017-0009-4.

9 Udalov A.A., Parshin S.V., Udalov A.V. (2018) Theoretical investigation of the effect of the taper angle of the deforming roller on the limiting degrees of deformation in the process of flow forming. *MATEC Web of Conferences*, 224, 01040. DOI: 10.1051/matecconf/201822401040.

10 Udalov A.A., Parshin S.V., Udalov A.V. (2019) Influence of the profile radius of the deforming roller on the limit degree of deformation in the process of flow forming. *Materials Science Forum*, 946, 800 – 806. DOI:10.4028/www.scientific.net/msf.946.800.

11 Okulov R.A., Semenova N.V. (2019) Modeling the Drawing of Square-Cross-Section Pipes/Tubes Made from Various Materials. *Metallurgist*, 65, 571-577. Available at: https://link.springer.com/article/10.1007/s11015-021-01192-z.

12 Hatala M., Botko F., Peterka J., Bella P., Radic P. (2020) Evaluation of strain in cold drawing of tubes with internally shaped surface. *Materials Today: Proceedings*, 22, 287 – 292. Available at: https://www.sciencedirect.com/science/article/abs/pii/S2214785319330962

13 Boutenel F., Delhomme M., Velay V., Boman R. (2018) Finite element modelling of cold drawing for high-precision tubes. *Comptes Rendus – Mecanique,* 346, 665 – 677. Available at: https://www.sciencedirect.com/science/article/pii/S1631072118301220

14 Vorontsov A.L. (2014) Theory and calculations of metal forming processes. Vol. 2. Moscow, BMSTU Publ., 441. Available at the: https://www.labirint.ru/books/541059/ [in Russian]

15 Vinnik P.M., Ivanov K.M., Danilin G.A., Remshev E.Yu., Vinnik T.V. (2015) Prediction of the mechanical properties of a part obtained by drawing with thinning. *Metalloobrabotka*, 88, 31 – 36. Available at: https://polytechnics.ru/arhmo/2015/product-details/365-metalloobrabotka-4-88-2015.html.

AUTHORS' INFORMATION

Rasulov, Zainodin Nurmukhamedovich – Candidate of Technical Sciences, Head of the Youth Laboratory, BSTU "VOENMEKH" named after D.F.Ustinova, Saint Petersburg, Russia; ORCID 0000-0002-6966-7060; rasulov_zn@voenmeh.ru

Olehver, Alexey Ivanovich – Candidate of Technical Sciences, Associate Professor, BSTU "VOENMEKH" named after D.F. Ustinova, BSTU "VOENMEKH" named after D.F. Ustinova, Saint Petersburg, Russia; ORCID 0009-0003-8630-344X; leshicher@mail.ru

Remshev, Evgenii Uri'evich – Candidate of Technical Sciences, Associate Professor, BSTU "VOENMEKH" named after D.F. Ustinova, Saint Petersburg, Russia; ORCID 0000-0002-7630-0398; remshev@mail.ru

Voinash, Sergey Aleksandrovich – Master, Leading Engineer, Research laboratory "Intelligent Mobility", Institute of Design and Spatial Arts, Kazan Federal University, Kazan, Russia; Scopus ID : 57194339935; ORCID: 0000-0001-5239-9883; sergey_voi@mail.ru

Vornacheva, Irina Valerievna – Candidate of Technical Sciences, Associate Professor, South-West State University, Kursk, Russia; ORCID: 0009-0003-5511-235X; vornairina2008@yandex.ru

Sokolova, Viktoriia Alexandrovna – Candidate of Technical Sciences, Associate Professor, Leading Researcher, Research Laboratory "Intelligent Mobility", Institute of Design and Spatial Arts, Kazan Federal University, Kazan, Russia; ORCID iD: 0000-0001-6880-445X; sokolova_vika@inbox.ru

Malikov, Vladimir Nickolaevich – Candidate of Technical Sciences, Associate Professor, Department of General and Experimental Physics, Altai State University, Barnaul, Altai Territory, Russia; ORCID iD: 0000-0003-0351-4843; osys11@gmail.com